journal

J. Am. Ceram. Soc., **84** [11] 2638–44 (2001)

Microstructure and Mechanical Properties of Porous Alumina Ceramics Fabricated by the Decomposition of Aluminum Hydroxide

Zhen-Yan Deng, Takayuki Fukasawa,* and Motohide Ando

Synergy Ceramics Laboratory, Fine Ceramics Research Association, Nagoya 463-8687, Japan

Guo-Jun Zhang* and Tatsuki Ohji*

Synergy Materials Research Center, National Institute of Advanced Industrial Science and Technology, Nagoya 463-8687, Japan

The mechanical properties of Al_2O_3-based porous ceramics fabricated from pure Al_2O_3 powder and the mixtures with $Al(OH)_3$ were investigated. The fracture strength of the porous Al_2O_3 specimens sintered from the mixture was substantially higher than that of the pure Al_2O_3 sintered specimens because of strong grain bonding that resulted from the fine Al_2O_3 grains produced by the decomposition of $Al(OH)_3$. However, the elastic modulus of the porous Al_2O_3 specimens did not increase with the incorporation of $Al(OH)_3$, so that the strain to failure of the porous Al_2O_3 ceramics increased considerably, especially in the specimens with high porosity, because of the unique pore structures related to the large original $Al(OH)_3$ particles. Fracture toughness also increased with the addition of $Al(OH)_3$ in the specimens with higher porosity. However, fracture toughness did not improve in the specimens with lower porosity because of the fracture-mode transition from intergranular, at higher porosity, to transgranular, at lower porosity.

I. Introduction

POROUS ceramics are widely used as filters, sensors, and catalyst supports, as well as lightweight structural components. Usually, these porous materials are fragile, and their mechanical properties are inferior to those of the corresponding dense materials. Improvement of the mechanical properties of porous ceramics is an important issue for increasing their reliability in practical applications.

Usually, the mechanical properties of porous ceramics are related to such factors as pore volume fraction, pore structures, and grain bonding of the matrix grains. Optimizing pore structures represents an effective way of improving the mechanical properties of porous ceramics. For example, Shigegaki *et al.*[1] used tape-casting to fabricate porous Si_3N_4 with an anisotropic configuration of grains and pores and found that the strain-to-failure of the Si_3N_4 was appreciably increased. Liu[2] used different-sized poly(vinyl butyral) particles as pore-forming agents to fabricate porous hydroxyapatite ceramics, and his results showed that specimens with small macropores exhibited higher strength than those with large macropores.

Porous Al_2O_3 ceramics have attracted considerable attention for many years because of their good thermal stability at elevated temperatures. Traditional methods for fabricating porous Al_2O_3 ceramics for structural applications include partially sintering Al_2O_3 powder[3–7] and forming the porous structures by adding fugitives to the starting powder.[8,9] Green and coworkers[4,5] found that before any densification occurs, the formation of necks between touching particles by surface diffusion can increase the elastic modulus to ~10% of the fully dense value. Ostrowski and Rödel[7] found that a small uniaxial pressure during densification has almost no effect on the relationship between strength and porosity in Al_2O_3 ceramics. Lyckfeldt and Ferreira[9] fabricated porous Al_2O_3 materials by a starch-consolidation method and obtained high-porosity Al_2O_3. Recently, some new ways to fabricate porous Al_2O_3 ceramics, such as by pulse electric current sintering (PECS)[10] and by the reaction bonding of Al_2O_3 (RBAO)[11,12] from an Al_2O_3/aluminum mixture have been developed. Oh *et al.*[10] found that PECS could enhance grain neck growth and increase the fracture strength of porous Al_2O_3 and Al_2O_3–SiC nanocomposites. Claussen *et al.*[11] found that strong grain bonding could be obtained by RBAO, because the strength of porous Al_2O_3 fabricated by RBAO was appreciably higher than that fabricated by partial sintering.

In the present study, a mixture of α-Al_2O_3 and $Al(OH)_3$ was used as the starting powder. Because $Al(OH)_3$ experiences a 60% volume contraction during decomposition and produces fine Al_2O_3 grains, porous Al_2O_3 ceramics with high porosity and strong grain bonding should be obtainable.[13] On the other hand, pore structures are modified by the addition of $Al(OH)_3$ when the partial-sintering method is used, because the pore morphology is related in some way to the shape of the original $Al(OH)_3$ particles. The goal of this research was to optimize pore structures and strengthen grain bonding to improve the mechanical properties of porous Al_2O_3 ceramics.

II. Experimental Procedure

Highly pure α-Al_2O_3 (99.99%, 0.21 μm, TM-DAR, Tamei Chemical Co., Nagano, Japan) and $Al(OH)_3$ (99.99%, 2.5 μm, High Purity Chemical Co., Tokyo, Japan) were used in the present experiment. Two types of starting powders were prepared: Al_2O_3 and Al_2O_3 + $Al(OH)_3$, referred to as A and AH, respectively.

The processing route for this work was the same as that in a previous study.[14] Green-body billets with a relative density of 53% were prepared by cold-pressing and then sintered in a furnace with an air atmosphere. The heating rate was set to 1°C/min at <1000°C, and 10°C/min at >1000°C for the $Al(OH)_3$-containing billets, so that the decomposition of $Al(OH)_3$ would be complete before sintering began. A heating rate of 10°C/min was used for the pure Al_2O_3 billets. All specimens were held at the sintering temperature for 30 min and then cooled to room temperature at a rate of 10°C/min. Different sintering temperatures were used to get

J. Rödel—contributing editor

Manuscript No. 188448. Received August 3, 2000; approved June 27, 2001.
Supported by METI, Japan, as part of the Synergy Ceramics Project. Supported in part by NEDO. The authors are members of the Joint Research Consortium of Synergy Ceramics.
*Member, American Ceramic Society.

different porosity specimens, as shown in Fig. 1, where the number after AH represents the volume percentage of $Al(OH)_3$ in the starting mixtures; e.g., AH60 represents 60 vol% $Al(OH)_3$ in the mixture. As the decomposition of $Al(OH)_3$ produces 60% volume contraction, the porosity of the $Al(OH)_3$-containing billets is greater than in the pure Al_2O_3 billets before sintering, and the AH billets required a higher sintering temperature to reach the same density as that of the pure Al_2O_3 billets.[15,16]

The sintered specimens were cut into pieces measuring 3 mm × 4 mm × 40 mm, and then ground and beveled before strength and toughness measurements. Strength was determined by three-point bend tests, with a span of 30 mm and a crosshead speed of 0.5 mm/min. Fracture toughness was measured using the single-edge notched-beam test,[17] with a notch depth of ~2.0 mm and a notch width of 0.1 mm. A span of 16 mm of the three-point bend test was used for strength measurement of the toughness specimens. Six specimens were used for each strength or toughness point. Young's modulus of the porous Al_2O_3 was measured by the pulse-echo method (Model No. 5052 PRX50 Pulser Receiver, Panametrics, Inc., Waltham, MA), according to JIS R1602. The data for Young's modulus represent an average of two or three specimens.

The pore-size distribution of the sintered porous Al_2O_3 specimens was measured by mercury intrusion porosimetry (Model No. Autopore 9220, Shimadzu Corp., Kyoto, Japan). The density of the sintered specimens was measured by the Archimedes method. The morphology and pore structures of the porous Al_2O_3 were observed, using the fresh-fractured surface of the sintered specimens, by SEM.

III. Results and Discussion

(1) Fracture Strength

The relationship between the bending strength and the relative density of porous Al_2O_3 ceramics prepared from different powders is shown in Fig. 2. Adding an increasing amount of $Al(OH)_3$ to the starting powder increased the bending strength of the porous Al_2O_3 appreciably, especially for the specimens with high porosity, compared with those of the same porosity prepared from pure Al_2O_3 powder. For example, the specimens prepared from AH90 powder had higher strength than those prepared from AH60, as shown in Fig. 2(b). The maximum porosity of the porous Al_2O_3 treated by the present method was as high as 62%, and a bending strength as high as 50 MPa at 50% porosity was obtained.

The reinforcing mechanism for increasing the bending strength of porous Al_2O_3 by adding $Al(OH)_3$ to the starting powder is the strong interface bonding between the grains produced by the decomposition of $Al(OH)_3$, discussed later. In fact, the decomposition of $Al(OH)_3$ formed very fine Al_2O_3 grains,[14] which have a higher activity than ordinary Al_2O_3 grains and can produce good bonding; similar results have been found by Claussen *et al.*[11] Figure 3 shows the pore and grain morphologies of porous Al_2O_3 specimens with higher porosity prepared from pure Al_2O_3 and $Al(OH)_3$-containing powders, indicating that the bonding area between the Al_2O_3 grains in the AH specimens apparently was larger than that in pure Al_2O_3 sintered specimens with comparable porosity.

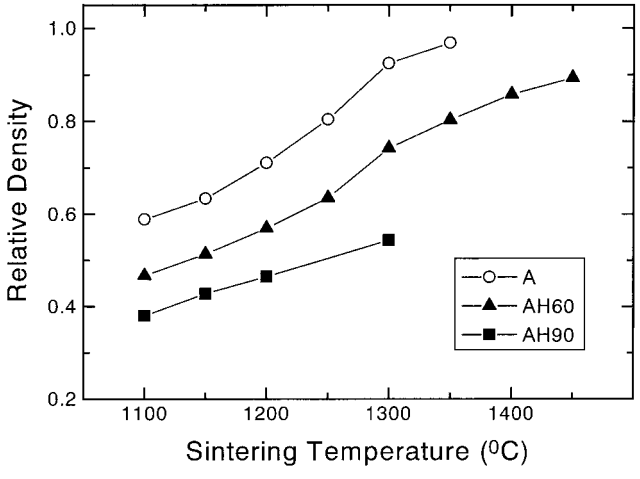

Fig. 1. Dependence of relative density on the sintering temperature for the specimens prepared from different starting powders.

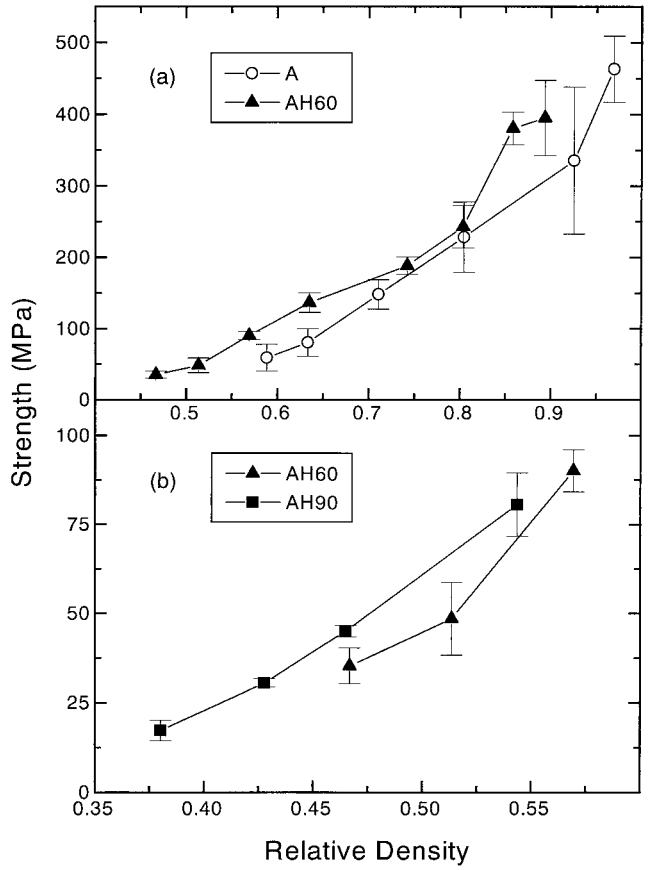

Fig. 2. Dependence of bending strength on the relative density of porous Al_2O_3 ceramics prepared from (a) A and AH60 powders and (b) AH60 and AH90 powders for the sintered specimens with high porosity.

(2) Elastic Modulus

The dependence of Young's modulus on the relative density of porous Al_2O_3 ceramics prepared from different powders is shown in Fig. 4(a). For comparison, the results of Lam *et al.*[3] are also added, where $\rho_0 = 0.62$ and $\rho_0 = 0.50$ represent the initial relative densities of the two types of Al_2O_3 compacts used by those researchers. Unlike the fracture strength, which was dependent on the porosity, the elastic modulus of the porous Al_2O_3 did not increase with the addition of $Al(OH)_3$ to the starting powder. Because the fracture strength increased and the elastic modulus did not increase, the strain to failure (bending strength divided by Young's modulus) increased with the addition of $Al(OH)_3$ to the starting powder, especially for the high-porosity specimens, as compared with the results for the porous Al_2O_3 prepared from pure Al_2O_3 powders, as shown in Fig. 4(b). High strain to failure implies high reliability and good thermal-shock resistance in application.[1]

Lam *et al.*[3] sintered porous Al_2O_3 ceramics by using two types of pure Al_2O_3 compacts with different initial densities, and found that the sintering temperature and fracture strength of porous Al_2O_3 increased as porosity increased in the initial compact, a finding similar to our present results. However, the elastic modulus also increased as the compact porosity increased (Fig. 4(a)), so that

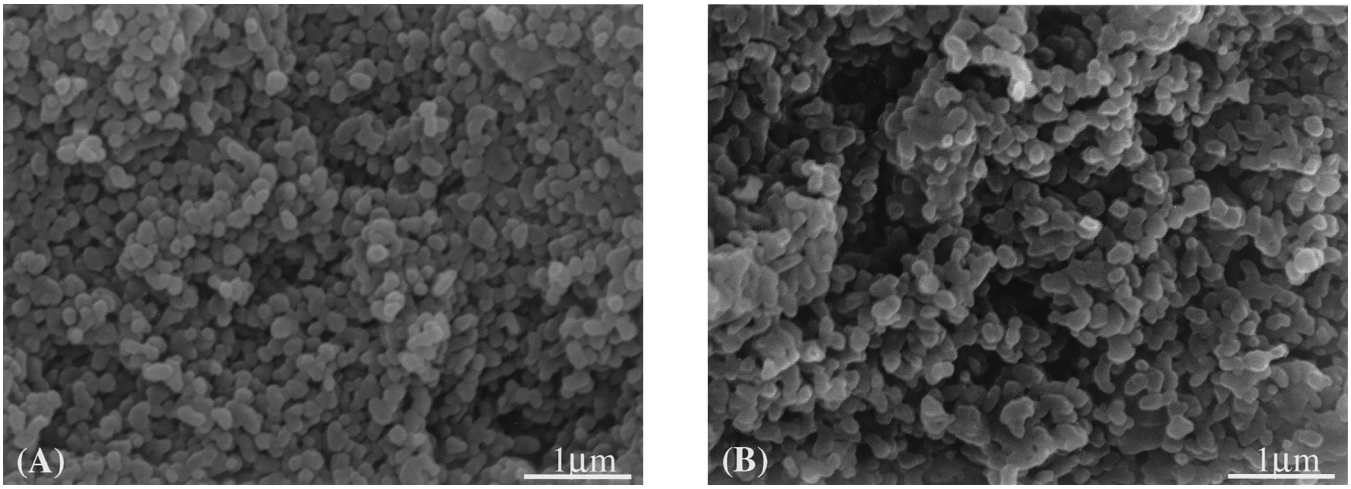

Fig. 3. SEM micrographs of the fracture surfaces of the porous Al_2O_3 specimens prepared from (a) pure Al_2O_3 powder and sintered at 1100°C (porosity 41.14%) and (b) AH60 powder and sintered at 1200°C (porosity 43.07%).

the strain to failure of the porous Al_2O_3 fabricated by Lam *et al.*[3] exhibited no improvement (Fig. 4(b)). The above results indicate that the effect of initial compact porosity before sintering on the elastic modulus of porous Al_2O_3 ceramics differs for pure Al_2O_3 and $Al(OH)_3$-containing billets.

The low elastic modulus in porous Al_2O_3 ceramics sintered from $Al(OH)_3$-containing powder originates from their unique pore morphology and microstructure, because different grain and pore arrangement results in a different relationship of elastic modulus to porosity.[18–21] Actually, the pore shape and structures in the AH specimens are in some way related to the original shape of the $Al(OH)_3$ particles, because the morphology of the $Al(OH)_3$ particle is retained after the $Al(OH)_3$ particles have decomposed into Al_2O_3 grains.[14]

Figure 5 is a schematic representation of the pore morphologies of the pure Al_2O_3 and the $Al(OH)_3$-containing billets during sintering. A spherical shape is assumed for the $Al(OH)_3$ particles, because no special shape was observed.[14] Because the average $Al(OH)_3$ particle (2.5 μm) was much larger than the Al_2O_3 grains produced by $Al(OH)_3$ decomposition and the added Al_2O_3 grains (0.21 μm), the pore structures in the AH specimens can be viewed as the stacking of large solid spheres that, in turn, are constructed

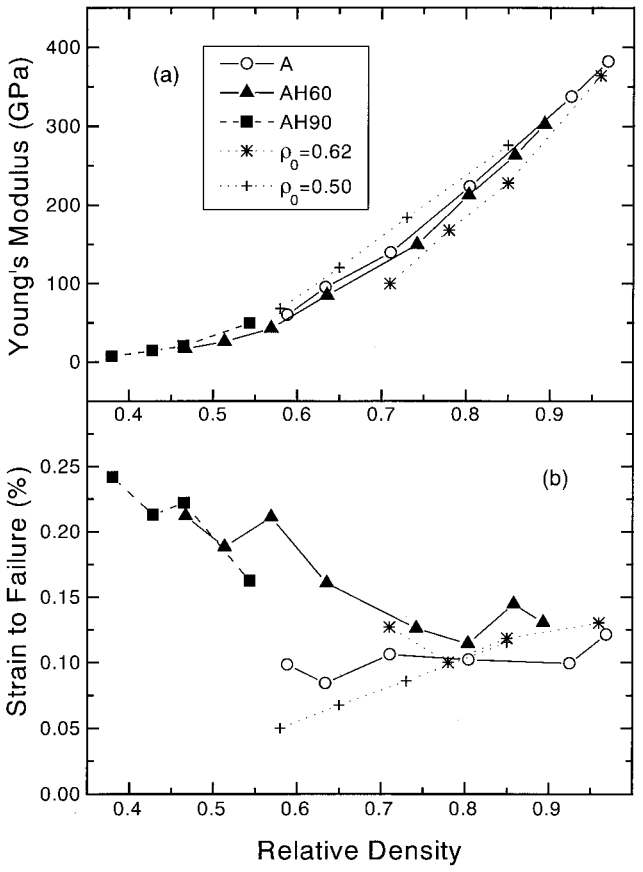

Fig. 4. Dependence of (a) Young's modulus and (b) strain to failure on the relative density of porous Al_2O_3 ceramics prepared from different powders.

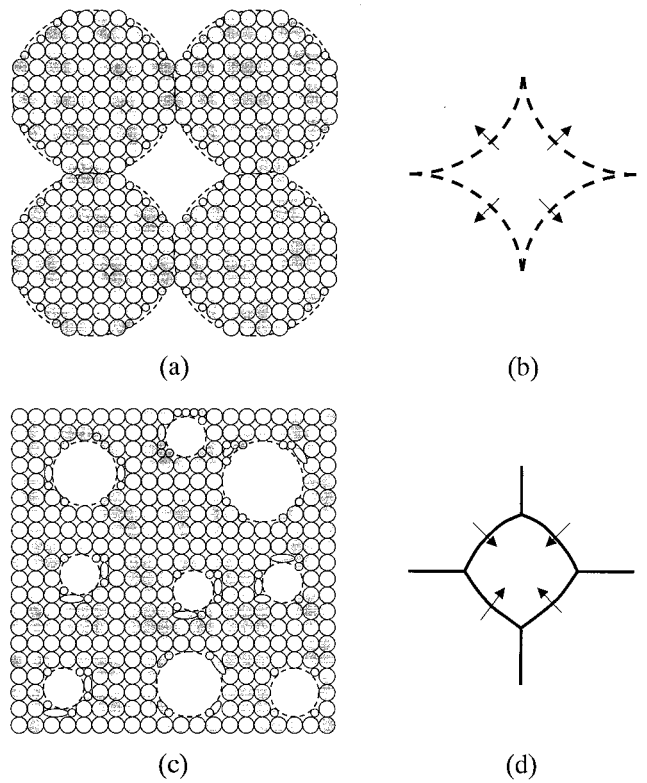

Fig. 5. Two-dimensional schematic representation of (a) general pore morphology, (b) the main pore channel related to $Al(OH)_3$ particles in the $Al(OH)_3$-containing billets, (c) general pore morphology, and (d) the main pore channel in the pure Al_2O_3 prepared billets during sintering.

of another stacking of small Al_2O_3 grains (Fig. 5(a)). Such pore morphology was evident in the AH specimens with high porosity, as shown in Fig. 3(b). Of course, the small initial Al_2O_3 grains would fill part of the space of the large pores between $Al(OH)_3$ particles, depending on the volume percentage of Al_2O_3 grains in the initial mixtures,[13,22] but the basic pore structures should be similar to those in Fig. 5(a). The bimodal pore structure in the AH specimens was also demonstrated by their pore size distributions (see Fig. 6 of Ref. 14).

The pore morphology of the porous Al_2O_3 prepared from pure Al_2O_3 powders differs from that of the AH specimens. Usually, some volume percentage of large spherical pores can exist in the initial pure Al_2O_3 green compacts, depending on the initial green-compact density, because of the nonuniform particle arrangement. From the viewpoint of mechanical stability, the spherical pores are more stable than the large pores of other shapes during cold pressing. This fact is shown in Fig. 5(c), and can be observed in the pure Al_2O_3 sintered specimen with high porosity (Fig. 3(a)). Of course, the higher the porosity of the green compact, the greater the volume percentage of large spherical pores in the pure Al_2O_3 sintered porous specimen.

The unique pore structures in the AH specimens were further confirmed by the change in their peak pore size, which represents the diameter of the pore channels between the large solid spheres.[14] Figure 6 shows that the peak pore size of the AH60 specimens increased during densification. However, the peak pore size of the pure Al_2O_3 sintered specimens decreased as the densification progressed.

According to the sintering theory,[23,24] there is a critical coordinate number, N_c, of grains around a pore during sintering. When the coordinate number, N, is $>N_c$, the pore is stable and grows, but if $N < N_c$, the pore contracts. The increase in peak pore size during densification for the AH60 specimens is related to the large coordinate number of the grains around the pores between the large solid spheres. Figure 5(b) shows that a boundary movement of the large pores in the AH specimens also accompanies the change of pore shape and size, which indicates the difficulty of increasing the necking area between the large solid spheres. The small solid contact area means a small elastic modulus.[18–20] The situation of the pure Al_2O_3 sintered specimens is different, because the coordinate number of the grains around the pores between the Al_2O_3 grains is small, so that the size of the main pore channels always decreases during densification, as shown in Fig. 5(d). This situation also implies that the large spherical pores in pure Al_2O_3 sintered specimens are isolated.

The relationship between the porosity and the elastic modulus of porous ceramics has been studied by many researchers,[3–5,18–20,25–31] and numerous models and formulas have been proposed to explain and fit the experimental data. The simplest empirical equation is[32,33]

$$E = E_0 \exp(-bP) \tag{1}$$

where E_0 is the zero-porosity Young's modulus, P the porosity, and b a characteristic constant. Although Eq. (1) is entirely empirical, not based on theory, it is the best fit to the experimental data.[34] In fact, the characteristic constant b is related to the particle stacking and pore shape.[19] Rice[20] used a minimum solid area (MSA) model to calculate the relationship of the elastic modulus to porosity for different particle and pore stacking, and then fitted the theory data by Eq. (1). He found that different particle and pore stacking have different b values (Fig. 4 of Ref. 20); e.g., solid spheres in cubic stacking (SSCS) correspond to $b \approx 5$, and spherical pores in cubic stacking (SPCS) have a value of $b \approx 3$.

Because the pore structures in porous Al_2O_3 ceramics prepared from pure Al_2O_3 and $Al(OH)_3$-containing powders can be viewed as one type of pore or particle stacking (PS1), with the matrix constructed by the other particle stacking (PS2), then,

$$\begin{aligned} E &= E_0' \exp(-b_1P_1) \\ &= E_0 \exp\left(-\frac{b_2P_2}{1-P_1}\right)\exp(-b_1P_1) \\ &= E_0 \exp\left(-b_1P_1 - \frac{b_2P_2}{1-P_1}\right) \end{aligned} \tag{2}$$

where $P_1 = V_1/V_t$ and $P_2 = V_2/V_t$ are the porosity in PS1 and PS2, respectively, with V_1 and V_2 the pore volume in PS1 and PS2, respectively, and V_t the total specimen volume; b_1 and b_2 are the characteristic constants of PS1 and PS2, respectively. The effective characteristic constant, b, of the porous Al_2O_3 ceramic can be obtained as follows:

$$b = \frac{b_1P_1 + b_2P_2/(1-P_1)}{P} \tag{3}$$

where $P = P_1 + P_2$ is the total porosity of the specimen. If the characteristic constants of PS1 and PS2 are equal, $b_1 = b_2 = b_0$, then

$$b = b_0 + \frac{b_0P_1P_2}{(1-P_1)(P_1+P_2)} > b_0 \tag{4}$$

This equation indicates that the elastic modulus of porous ceramics, which consists of one large agglomerate or pore stacking with the matrix constructed by the same type of particle or pore stacking, is always lower than that of porous ceramics with only single-modal particle or pore stacking. In fact, the above conclusions are drawn based on the minimum solid area, because Eq. (1) is a good approximation of minimum solid area in porous ceramics.[20,34] It is believed that Eq. (4) reflects the internal physical properties of porous ceramics with bimodal pore structures.

If the above situation is true for the AH specimens, it is easy to understand why the elastic modulus of those specimens is not larger than that of pure Al_2O_3 sintered specimens with a similar initial green density (Fig. 4(a)). The dependence of b on the porosity ratio of two stackings is shown in Fig. 7. If two stackings of PS1 and PS2 are the same, the effective constant is always larger than that of single-modal stacking, depending on the total porosity. If two stackings are different, the effective constant usually is located between the value of b_1 and b_2, depending on the porosity ratio and total porosity.

The b value of the porous Al_2O_3 ceramics sintered from different powders has been obtained by fitting the experimental data in Fig. 4(a) with Eq. (1) and is given in Table I, where the Young's modulus of dense Al_2O_3 is $E_0 = 400$ GPa.[3] Because the pore structures in the AH specimens can be viewed as a large

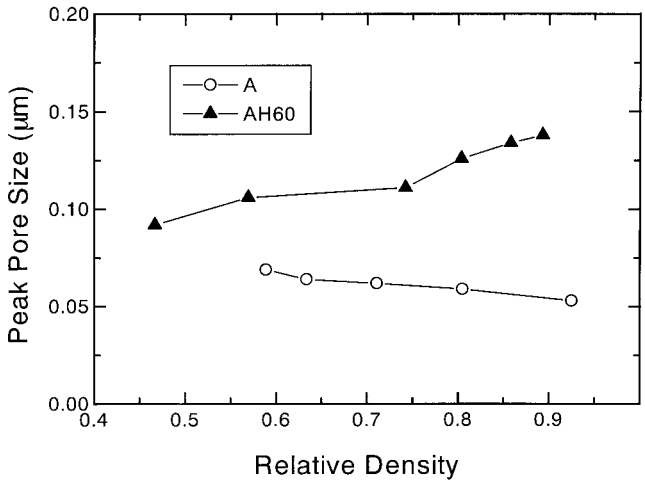

Fig. 6. Dependence of peak pore size on the relative density of the porous Al_2O_3 ceramics prepared from A and AH60 powders.

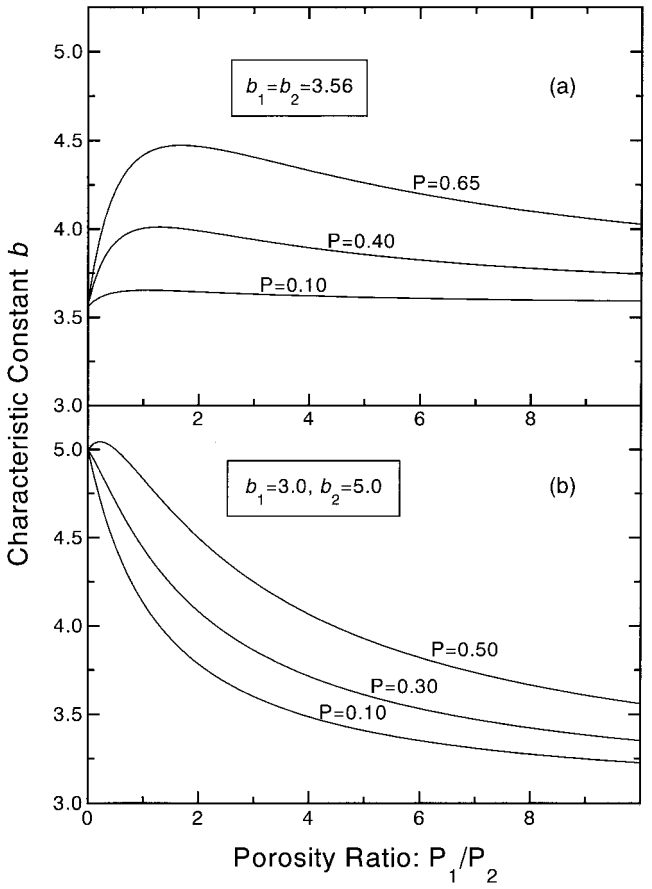

Fig. 7. Dependence of the effective characteristic constant b on the porosity ratio of two particle or pore stackings (a) $b_1 = b_2 = 3.56$ (pure Al_2O_3 sintered ceramics with initial green density $\rho_o = 0.53$) and (b) $b_1 = 3.0$ (SPCS) and $b_2 = 5.0$ (SSCS) in porous ceramics with different total porosity.

sphere stacking, with the matrix constructed of a similar small-grain stacking, and the characteristic constant of AH60 is larger than that of a pure Al_2O_3 sintered specimen with a similar green density ($\rho_0 = 0.53$), in accord with the prediction in Fig. 7(a).

On the other hand, decreasing the initial green density would increase the volume percentage of large pores in the green compacts,[35] because the porosity for a definite particle stacking is a constant and the matrix particle stacking without large pores can be viewed as a stable array; therefore, the volume percentage of large pores in the pure Al_2O_3 sintered specimens increases and the porosity ratio of the large pore stacking to the Al_2O_3 grain stacking would increase. If the large pore stacking is viewed as SPCS and the Al_2O_3 grain stacking as SSCS, the characteristic constant of the pure Al_2O_3 sintered specimens would decrease as the green density decreased, as listed in Table I. This suggestion is in good agreement with the theoretical prediction in Fig. 7(b). Because the pore shape and particle stacking will change during sintering, it is difficult to evaluate quantitatively the exact pore volume ratio of different stackings in porous Al_2O_3 specimens.

Table I. Characteristic Constant of Porous Al_2O_3 Ceramics Prepared from Different Powders

Starting powder	Characteristic constant, b
$\rho_0 = 0.62$	4.06
A, $\rho_0 = 0.53$	3.56
$\rho_0 = 0.50$	3.24
AH60	3.90
SSCS	~5
SPCS	~3

(3) Fracture Toughness

The dependence of fracture toughness (K_{IC}) on the relative density of porous Al_2O_3 ceramics prepared from different powders is shown in Fig. 8. The fracture toughness of porous Al_2O_3 increases with the addition of $Al(OH)_3$ to the starting powder only for specimens with higher porosity, compared with the pure Al_2O_3 sintered specimens. Also, the fracture toughness increases as the volume percentage of $Al(OH)_3$ in the starting powder increases (Fig. 8(b)). At lower porosity, the fracture toughness does not improve with the addition of $Al(OH)_3$. This phenomenon could be attributed to fracture-mode transition from intergranular, for the higher-porosity AH specimens, to transgranular, for the lower-porosity specimens, as shown in Figs. 3(b) and 9(b). For pure Al_2O_3 sintered specimens, the fracture mode is always intergranular, independent of the porosity (Figs. 3(a) and 9(a)). Relative to intergranular fracture, transgranular fracture in the low-porosity AH specimens probably reduces the crack deflection and decreases the critical strain energy release rate.

Transgranular fracture in the AH specimens at lower porosity probably results from the defects formed in the Al_2O_3 grains during sintering, because the bimodal stacking in the AH billets would result in nonuniform sintering driving stress and a resultant nonuniform shrinkage strain inside and near the surface of the large solid spheres related to the original $Al(OH)_3$ particles.[22,23,36–38]

(4) Reinforcing Mechanism

The elastic properties of porous ceramics, such as Young's modulus, are proportional to the minimum solid contact area

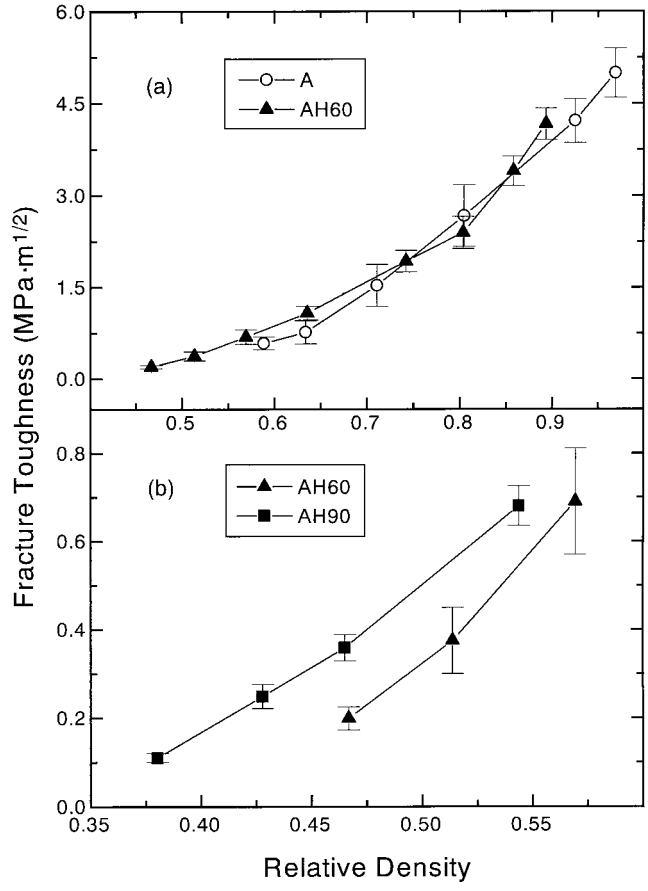

Fig. 8. Dependence of fracture toughness (K_{IC}) on the relative density of porous Al_2O_3 ceramics prepared from (a) A and AH60 powders and (b) AH60 and AH90 powders for the sintered specimens with high porosity.

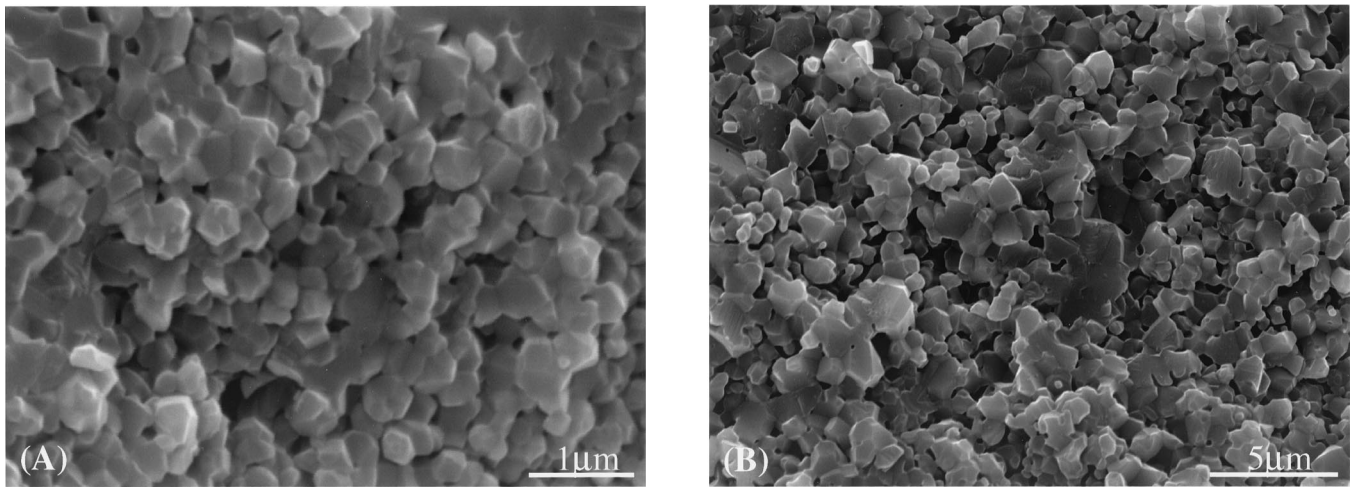

Fig. 9. SEM micrographs of the fracture surfaces of the porous Al_2O_3 specimens prepared from (a) pure Al_2O_3 powder and sintered at 1300°C (porosity 7.5%) and (b) AH60 powder and sintered at 1450°C (porosity 10.7%).

between the ceramic particles.[20,34,35,39] If the spherical particles are considered and the particle stacking is a cubic array, the minimum solid area is the necking area between the particles, i.e., the grain bonding area. If the particle stacking isn't the cubic array, the minimum solid area is a representation of the grain bonding area. Because Young's modulus is an internal physical property of ceramic materials, it is independent of surface defects.

The strength of porous ceramics is also related to the minimum solid area.[20,34,35] However, there are other possible factors that affect the strength, such as surface defects. Recently, Flinn *et al.*[40] studied the evolution of defect size and strength of porous Al_2O_3 during sintering and found that the size of surface defects has only a negligible influence on the strength of porous ceramics, provided the defect size is large compared with the microstructural features. Those experimental results showed that porous Al_2O_3 ceramics with different-sized surface defects and different matrix grain sizes follow the same strength-porosity relationship. In fact, the defect-stress concentration effects on mechanical properties of porous ceramics are limited because of the pore-stress interactions,[41] especially for the porous materials with high porosity, and by bending tests. Therefore, if there are no other reinforcing mechanisms, the strength of porous ceramics is also determined by the minimum solid area. The pore structures in the present Al_2O_3 specimens are very fine, similar to those fabricated by Flinn *et al.*;[40] the surface defect effects on the bending strength could be neglected.

Because the fracture mode was intergranular for the high-porosity Al_2O_3 specimens, the bonding interface should be the most stress-concentrated place, and its area could be viewed as a representation of the minimum solid area. The nominal interface bonding strength can be evaluated by

$$\sigma_{\text{bonding}} \propto \frac{P_{\text{load}}}{S_{\min}} = \left(\frac{P_{\text{load}}}{S_0}\right)\left(\frac{S_0}{S_{\min}}\right) = \sigma_f\left(\frac{E_0}{E}\right) = E_0\varepsilon_f \tag{5}$$

where P_{load} is the applied load, $S_{\min}$ and S_0 are the minimum solid area and the total cross-section area, respectively, and σ_f and ε_f are the fracture strength and the strain to failure of Al_2O_3 specimens, respectively. Equation (5) implies that the strain to failure of the porous ceramics is that of the bonding interface. Because the strain to failure of the AH specimen is apparently larger than that of the pure Al_2O_3 sintered specimen at high porosity (Fig. 4(b)), the grain bonding between the Al_2O_3 grains produced by the $Al(OH)_3$ decomposition is stronger than that between the initial Al_2O_3 grains in the starting mixtures. In fact, the strong grain bonding by the $Al(OH)_3$ decomposition could be also known from the increase in fracture toughness for the high-porosity AH specimens.

IV. Conclusions

The mechanical properties of porous Al_2O_3 ceramics prepared from pure Al_2O_3 powder and the mixtures with $Al(OH)_3$ particles were investigated, with the following results:

(1) The fracture strength of porous Al_2O_3 ceramics increased with the addition of $Al(OH)_3$ to the starting powder because of strong grain bonding resulting from the fine Al_2O_3 grains produced by the decomposition of $Al(OH)_3$.

(2) Unlike the fracture strength, which was dependent on porosity, the elastic modulus of porous Al_2O_3 ceramics did not increase with the addition of $Al(OH)_3$, so that the strain to failure of the porous Al_2O_3 ceramics increased considerably. The decrease in the elastic modulus with the addition of $Al(OH)_3$ was a result of the unique pore microstructures related to the large original $Al(OH)_3$ particles in the porous Al_2O_3.

(3) The fracture toughness also increased with the addition of $Al(OH)_3$ in the higher-porosity Al_2O_3 ceramics. However, the addition of $Al(OH)_3$ caused no improvement in the fracture toughness of porous Al_2O_3 ceramics with lower porosity, because of the fracture-mode transition from intergranular, at higher porosity, to transgranular, at lower porosity.

Acknowledgment

The authors are grateful to Dr. You Zhou for invaluable discussion and Dr. Jian-Feng Yang for experimental assistance.

References

[1]Y. Shigegaki, M. E. Brito, K. Hirao, M. Toriyama, and S. Kanzaki, "Strain Tolerant Porous Silicon Nitride," *J. Am. Ceram. Soc.*, **80** [2] 495–98 (1997).

[2]D. M. Liu, "Influence of Porosity and Pore Size on the Compressive Strength of Porous Hydroxyapatite Ceramic," *Ceram. Int.*, **23**, 135–39 (1997).

[3]D. C. C. Lam, F. F. Lange, and A. G. Evans, "Mechanical Properties of Partially Dense Alumina Produced from Powder Compacts," *J. Am. Ceram. Soc.*, **77** [8] 2113–17 (1994).

[4]S. C. Nanjangud, R. Brezny, and D. J. Green, "Strength and Young's Modulus Behavior of a Partially Sintered Porous Alumina," *J. Am. Ceram. Soc.*, **78** [1] 266–68 (1995).

[5]D. Hardy and D. J. Green, "Mechanical Properties of a Partially Sintered Alumina," *J. Eur. Ceram. Soc.*, **15**, 769–75 (1995).

[6]T. Ostrowski, A. Ziegler, R. K. Bordia, and J. Rodel, "Evolution of Young's Modulus, Strength, and Microstructure during Liquid-Phase Sintering," *J. Am. Ceram. Soc.*, **81** [7] 1852–60 (1998).

[7]T. Ostrowski and J. Rödel, "Evolution of Mechanical Properties of Porous Alumina during Free Sintering and Hot Pressing," *J. Am. Ceram. Soc.*, **82** [11] 3080–86 (1999).

[8]D. A. Hirschfeld, T. K. Li, and D. M. Liu, "Processing of Porous Oxide Ceramics," *Key Eng. Mater.*, **115**, 65–79 (1996).

[9]O. Lyckfeldt and J. M. F. Ferreira, "Processing of Porous Ceramics by 'Starch Consolidation'," *J. Eur. Ceram. Soc.*, **18**, 131–40 (1998).

[10]S. T. Oh, K. I. Tajima, M. Ando, and T. Ohji, "Strengthening of Porous Alumina by Pulse Electric Current Sintering and Nanocomposite Processing," *J. Am. Ceram. Soc.*, **83** [5] 1314–16 (2000).

[11]N. Claussen, S. X. Wu, and D. Holz, "Reaction Bonding of Aluminum Oxide (RBAO) Composites: Processing, Reaction Mechanisms and Properties," *J. Eur. Ceram. Soc.*, **14**, 97–109 (1994).

[12]J. Luyten, T. V. Gestel, and E. Vanswijgenhoven, "Processing of Porous Ceramics"; pp. 17-B-3 in *7th International Conference on Ceramic Processing Science* (ICCPS) (Inuyama City, Aichi, Japan, 2000).

[13]S. Kwon and G. L. Messing, "Constrained Densification in Boehmite-Alumina Mixtures for the Fabrication of Porous Alumina Ceramics," *J. Mater. Sci.*, **33**, 913–21 (1998).

[14]Z. Y. Deng, T. Fukasawa, M. Ando, G. J. Zhang, and T. Ohji, "High-Surface-Area Alumina Ceramics Fabricated by the Decomposition of $Al(OH)_3$," *J. Am. Ceram. Soc.*, **84** [3] 485–91 (2001).

[15]R. L. Coble, "Sintering Crystalline Solids. I. Intermediate and Final State Diffusion Models," *J. Appl. Phys.*, **32** [5] 787–92 (1961).

[16]R. L. Coble, "Sintering Crystalline Solids. II. Experimental Test of Diffusion Models in Powder Compacts," *J. Appl. Phys.*, **32** [5] 793–99 (1961).

[17]D. Broek, *Elementary Engineering Fracture Mechanics*, 4th Ed.; p. 85. Martinus Nijhoff, The Hague, The Netherlands, 1986.

[18]F. P. Knudsen, "Dependence of Mechanical Strength of Brittle Polycrystalline Specimens on Porosity and Grain Size," *J. Am. Ceram. Soc.*, **42** [8] 376–87 (1959).

[19]R. W. Rice, "Comparison of Stress Concentration versus Minimum Solid Area Based Mechanical Property-Porosity Relations," *J. Mater. Sci.*, **28**, 2187–90 (1993).

[20]R. W. Rice, "Evaluation and Extension of Physical Property-Porosity Models Based on Minimum Solid Area," *J. Mater. Sci.*, **31**, 102–18 (1996).

[21]A. K. Mukhopadhyay and K. K. Phani, "An Analysis of Microstructural Parameters in the Minimum Contact Area Model for Ultrasonic Velocity-Porosity Relations," *J. Eur. Ceram. Soc.*, **20**, 29–38 (2000).

[22]S. Kwon and G. L. Messing, "Sintering of Mixtures of Seeded Boehmite and Ultrafine α-Alumina," *J. Am. Ceram. Soc.*, **83** [1] 82–88 (2000).

[23]F. F. Lange, "Sinterability of Agglomerated Powders," *J. Am. Ceram. Soc.*, **67** [2] 83–89 (1984).

[24]J. L. Shi, "Solid State Sintering of Ceramics: Pore Microstructure Models, Densification Equations and Applications," *J. Mater. Sci.*, **34**, 3801–12 (1999).

[25]E. A. Dean, "Elastic Moduli of Porous Sintered Materials as Modeled by a Variable-Aspect-Ratio Self-Consistent Oblate-Spheroidal-Inclusion Theory," *J. Am. Ceram. Soc.*, **66** [12] 847–54 (1983).

[26]J. C. Wang, "Young's Modulus of Porous Materials: Part 1, Theoretical Derivation of Modulus-Porosity Correlation," *J. Mater. Sci.*, **19**, 801–808 (1984).

[27]J. C. Wang, "Young's Modulus of Porous Materials: Part 2, Young's Modulus of Porous Alumina with Changing Pore Structure," *J. Mater. Sci.*, **19**, 809–14 (1984).

[28]K. K. Phani and S. K. Niyogi, "Young's Modulus of Porous Brittle Solids," *J. Mater. Sci.*, **22**, 257–63 (1987).

[29]K. K. Phani and S. K. Niyogi, "Elastic Modulus-Porosity Relation in Polycrystalline Rare-Earth Oxides," *J. Am. Ceram. Soc.*, **70** [12] C-362–C-366 (1987).

[30]N. Ramakrishnan and V. S. Arunachalam, "Effective Elastic Moduli of Porous Ceramic Materials," *J. Am. Ceram. Soc.*, **76** [11] 2745–52 (1993).

[31]G. Lu, G. Q. Lu, and Z. M. Xiao, "Mechanical Properties of Porous Materials," *J. Poro. Mater.*, **6**, 359–68 (1999).

[32]W. Duckworth, "Discussion of Ryshkewitch Paper," *J. Am. Ceram. Soc.*, **36** [2] 68 (1953).

[33]R. M. Spriggs, "Expression for Effect of Porosity on Elastic Modulus of Polycrystalline Refractory Materials, Particularly Aluminum Oxide," *J. Am. Ceram. Soc.*, **44** [12] 628–29 (1961).

[34]R. W. Rice, "Comparison of Physical Property-Porosity Behaviour with Minimum Solid Area Models," *J. Mater. Sci.*, **31**, 1509–28 (1996).

[35]R. W. Rice, "Evaluating Porosity Parameters for Porosity-Property Relations," *J. Am. Ceram. Soc.*, **76** [7] 1801–808 (1993).

[36]A. G. Evans, "Considerations of Inhomogeneity Effects in Sintering," *J. Am. Ceram. Soc.*, **65** [10] 497–501 (1982).

[37]C. H. Hsueh, A. G. Evans, R. M. Cannon, and R. J. Brook, "Viscoelastic Stress and Sintering Damage in Heterogeneous Powder Compacts," *Acta Metall.*, **34** [5] 927–36 (1986).

[38]L. C. De Jonghe, M. N. Rahaman, and C. H. Hsueh, "Transient Stresses in Bimodal Compacts during Sintering," *Acta Metall.*, **34** [7] 1467–71 (1986).

[39]A. P. Roberts and E. J. Garboczi, "Elastic Properties of Model Porous Ceramics," *J. Am. Ceram. Soc.*, **83** [12] 3041–48 (2000).

[40]B. D. Flinn, R. K. Bordia, A. Zimmermann, and J. Rodel, "Evolution of Defect Size and Strength of Porous Alumina during Sintering," *J. Eur. Ceram. Soc.*, **20,** 2561–68 (2000).

[41]R. W. Rice, "Limitations of Pore-Stress Concentrations on the Mechanical Properties of Porous Materials," *J. Mater. Sci.*, **32**, 4731–36 (1997). □